

X-RAY EMISSION FROM DEGENERATE DWARFS

N. D. Kylafis^{*}, D. Q. Lamb^{*+}, and A. R. Masters^{*}

^{*} Department of Physics
University of Illinois

⁺ Department of Physics
Massachusetts Institute of Technology

INTRODUCTION

Accreting degenerate dwarfs comprise an important class of galactic X-ray sources. This has become evident with the recent discovery of soft and hard X-ray emission from accreting magnetic degenerate dwarfs such as AM Her, AN UMa, and 2A0311-23, and from nonmagnetic or weakly magnetic cataclysmic variables such as SS Cyg, U Gem, EX Hya, and GK Per (for an observational review, see Garmire 1979). Previously known low mass X-ray binaries such as Cyg X-2 and Sco X-1, as well as some of the "bulge" sources, may also be moderate luminosity nonmagnetic degenerate dwarfs (Kylafis and Lamb 1979; Branduardi *et al.* 1979). Finally, theory predicts (Fabian, Pringle and Rees 1976; Katz 1977; Kylafis and Lamb 1979) an as yet undiscovered class of low luminosity nonmagnetic degenerate dwarf X-ray sources having hard ($T_{\text{obs}} \geq 30\text{-}50$ keV) spectra.

Here we review our recent theoretical studies of magnetic and non-magnetic degenerate dwarf X-ray sources (Kylafis and Lamb 1979; Lamb and Masters 1979; see also Kylafis *et al.* 1979). These studies indicate that the physical properties of X-ray sources (such as mass, magnetic field strength, and intrinsic luminosity) may be determined from the qualitative features of their X-ray spectra and from correlations between their X-ray luminosity and spectral temperature. Furthermore, in X-ray sources where the rotation period of the magnetic degenerate dwarf is not locked, as it is in AM Her, to the binary orbital period, our results suggest that X-ray and UV timing observations will eventually yield new information that is as exciting as that gained from timing observations of magnetic neutron stars.

QUALITATIVE PICTURE

A qualitative picture of X-ray emission by accreting degenerate dwarfs is the following. As accreting matter flows toward the star, a strong standoff shock forms far enough above the star for the hot, post-shock matter to cool and come to rest at the stellar surface (Hoshi 1973; Aizu 1973; Fabian, Pringle, and Rees 1976). The standoff distance $d = 1/4 v_{\text{ff}}(r_s) t_{\text{cool}}(r_s)$, where r_s is the shock radius, v_{ff} is the freefall velocity, and t_{cool} is the time scale for cooling, due to bremsstrahlung and, if a magnetic field is present, cyclotron emission. Roughly half of the bremsstrahlung flux is emitted outward and forms a hard X-ray component. Roughly half of the cyclotron flux is emitted outward and

forms a blackbody-limited component in the UV. The other halves of the bremsstrahlung and cyclotron fluxes are emitted inward and are reflected or absorbed by the stellar surface. The resulting blackbody flux forms a UV or soft X-ray component with $L_{bb} \approx L_{cyc} + L_{br}$, where L_{bb} , L_{cyc} , and L_{br} are the luminosities in the blackbody, cyclotron, and bremsstrahlung components.

If we allow for the possible presence of a magnetic field, then the accreting matter may be channeled onto the magnetic poles and accretion may occur over only a fraction f of the stellar surface. The effective accretion rate of the accreting sector is \dot{M}/f , and the corresponding luminosity is L/f . X and UV radiation from magnetic degenerate dwarfs is thus a function of stellar mass M , magnetic field strength B , and effective luminosity L/f . The dependence on stellar mass is significant but is less than on the other two variables. If we specify the mass of the star, the parameter regimes encountered are conveniently displayed on a $(B, L/f)$ -plane as shown for a $1 M_{\odot}$ star in Fig. 1. The upper left of the plane corresponds to low magnetic field strengths and high effective luminosities (and thus high densities in the emission region). In this portion of the plane, bremsstrahlung cooling dominates cyclotron cooling in the hot, post-shock emission region, and the character of the X-ray emission is essentially the same as that of a nonmagnetic degenerate dwarf. As one increases B or lowers L/f , moving toward the lower right in Fig. 1, cyclotron cooling becomes more important until eventually it dominates (Masters *et al.* 1977). The solid line shows the location at which this occurs for a $1 M_{\odot}$ star, as determined from detailed numerical calculations equating t_{cyc} and t_{br} , the cyclotron and bremsstrahlung cooling time scales. To the lower right of this solid line, the magnetic field qualitatively alters the character of the X-ray emission.

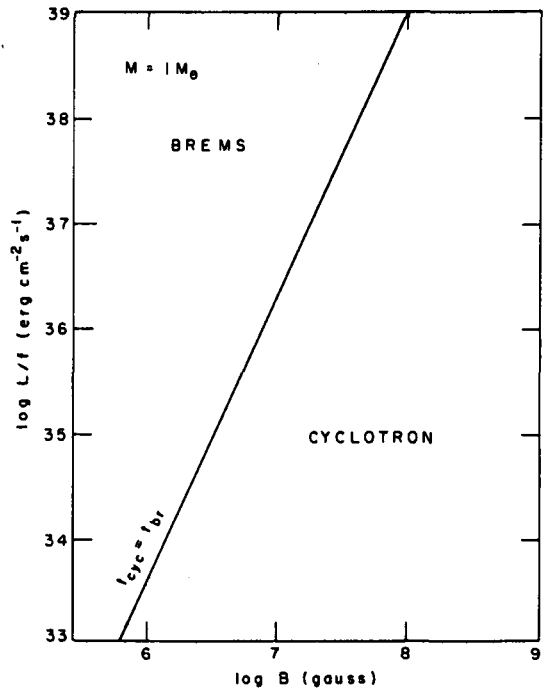


Fig. 1.- Parameter regimes in the $(B, L/f)$ -plane for a $1 M_{\odot}$ star. Cyclotron emission dominates below and to the right of the solid line, bremsstrahlung above and to the left.

STRONGLY MAGNETIC DEGENERATE DWARFS

The X and UV spectrum produced by accretion onto magnetic degenerate dwarfs generally has 4 components: 1) a blackbody-limited UV cyclotron component produced by the hot emission region, 2) a hard X-ray bremsstrahlung component also produced by the hot emission region, 3) a hard UV or soft X-ray blackbody component produced by cyclotron and bremsstrahlung photons that are absorbed by the stellar surface and re-emitted, and 4) secondary radiation from infalling matter above the shock or, possibly, from the stellar surface around the emission region. The first three components are clearly visible in Fig. 2, which shows spectra produced by hot, post-shock emission regions alone. Since the

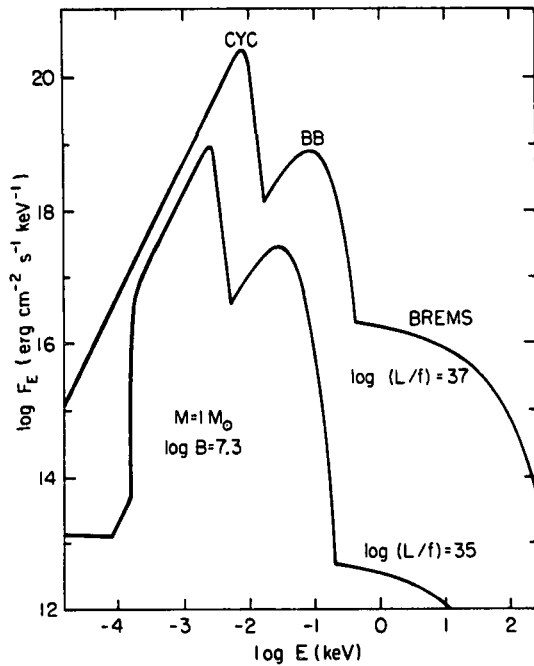


Fig. 2.- X-ray and UV spectra produced by two different accretion rates onto a $1 M_{\odot}$ star having a magnetic field of 2×10^7 gauss. The portion of each spectrum below ~ 5 eV is less certain due to possible secondary radiation. (From Lamb and Masters 1979. By permission of The Astrophysical Journal.)

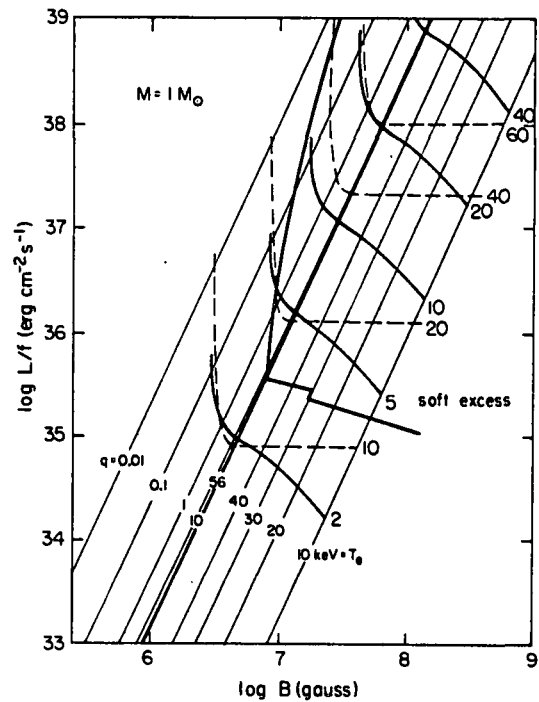


Fig. 3.- Temperature and luminosity contours in the $(B, L/f)$ -plane for a $1 M_{\odot}$ star. The heavy diagonal line marks the boundary between the bremsstrahlung and cyclotron regimes. The light diagonal lines are lines of constant q and T in keV. Numbers on the solid curves are E^* in eV. Numbers on the dashed lines are T_{bb} in eV. The spectral flux of the blackbody component exceeds that of the bremsstrahlung component at 0.25 keV to the right and above the heavy curve labeled "soft excess". (From Lamb and Masters 1979. By permission of The Astrophysical Journal.)

secondary radiation is not included, the spectra represent with relatively more uncertainty the actual observed spectrum below ~ 5 eV. Fig. 2 shows the X and UV spectra produced by accretion at two different rates, corresponding to $L/f = 10^{35}$ and 10^{37} erg s^{-1} , onto a $1 M_{\odot}$ star having a magnetic field of 2×10^7 gauss.

The spectra illustrated in Fig. 2 show that magnetic degenerate dwarfs are predicted to be strong UV sources with only a few percent of the total accretion luminosity ordinarily appearing as soft and hard X-rays, and therefore accessible to existing detectors.

The shapes and strengths of the spectral components are a function of both mass accretion rate and magnetic field strength. Spectral variations are therefore best displayed by plotting the contours of quantities of interest on a $(B, L/f)$ -plane. A set of such contours is shown in Fig. 3 for a $1 M_{\odot}$ star. Bremsstrahlung and cyclotron emission dominate in the same regions as in Fig. 1. Contours of constant E^* , the peak of the blackbody-limited cyclotron component, are shown as thick solid lines. Contours of constant T_{bb} , the temperature of the blackbody component, are shown as dashed lines. The thin solid

lines in the bremsstrahlung-dominated region show contours of constant $q = L_{\text{cyc}}/L_{\text{br}}$, while those in the cyclotron-dominated region show contours of constant T_e , the temperature of the bremsstrahlung hard X-ray component. To the upper right of the curve labeled "soft excess," the blackbody luminosity in soft X-rays exceeds the bremsstrahlung luminosity in hard X-rays.

Near and above $L/f = L_E = 1.4 \times 10^{38} \text{ erg s}^{-1}$, radiation pressure can be important and modify the results, but because photons can easily scatter out of the accretion column if $f \ll 1$, the Eddington luminosity does not represent the stringent upper limit to the luminosity that it does in the case of nonmagnetic degenerate dwarfs. Below and to the left of the curve $E^* = 2 \text{ eV}$, the assumption $d < R$ breaks down. In both of these regions, the values shown are expected to remain qualitatively correct.

Fig. 3 shows that observation of the qualitative features of the spectrum is generally sufficient to determine with relative confidence the physical conditions in the X-ray emission region, including the value of the magnetic field. As we have seen, the cyclotron component is ordinarily, and the blackbody component may frequently be, inaccessible to existing detectors. Nevertheless, optical, soft X-ray, and hard X-ray observations will often be sufficient to determine the mass and magnetic field of the star, and its accretion rate. For example, observation of T_e and T_{bb} fixes a point in the $(B, L/f)$ -plane of Fig. 3, and also constrains the star to a limited range of masses. Measurement of E^* , q , or a constraint from optical observations then tests the consistency, and hence validity, of the basic model. Furthermore, if an independent estimate of f exists, the intrinsic luminosity L is then known, as is the distance of the source.

NONMAGNETIC AND WEAKLY MAGNETIC DEGENERATE DWARFS

The X and UV spectrum produced by accretion onto nonmagnetic degenerate dwarfs generally has 3 components: 1) a hard X-ray bremsstrahlung component produced by the hot, post-shock emission region, 2) a soft X-ray blackbody component produced by bremsstrahlung photons that are absorbed by the stellar surface and re-emitted, and 3) secondary radiation produced by Compton heating of infalling matter above the shock.

These 3 components are clearly visible in Fig. 4 which shows the X and UV spectrum produced by accretion onto a $1 M_{\odot}$ star at a rate $0.15 \dot{M}_E$, corresponding to $\tau_{\text{es}} = 14$. At such accretion rates, the electron scattering optical depth τ_{es} from the emission region to infinity is large. The bremsstrahlung component is then degraded by Compton scattering, and the blackbody component contains an additional contribution from bremsstrahlung photons which are initially emitted outward, but which scatter, intercept the stellar surface, and are absorbed there. The secondary radiation, which is a consequence of such Compton scattering, is important only if degradation of the bremsstrahlung spectrum is substantial. Fig. 4 shows that degenerate dwarfs can produce larger luminosities than earlier estimates indicated, and even high mass stars can produce low temperature ($\leq 10 \text{ keV}$) X-ray spectra.

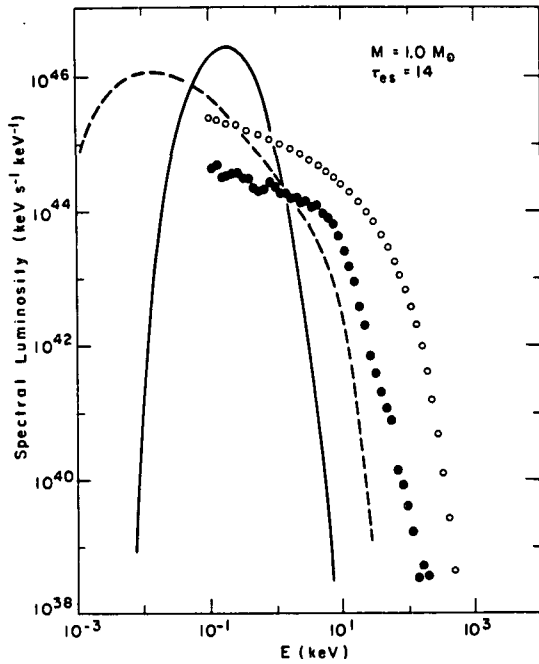


Fig. 4.- X-ray and UV spectrum produced by accretion onto a $1 M_{\odot}$ star at a rate $0.15 M_{\odot}$, corresponding to $\tau_{es} = 14$. Key: $\circ \circ \circ$ Spectrum produced by the emission region, $\bullet \bullet \bullet$ degraded spectrum observed at infinity, — blackbody spectrum emitted from the stellar surface, ---- secondary radiation produced by Compton heating. (From Kylafis and Lamb 1979. By permission of The Astrophysical Journal.)

At moderate and high accretion rates the spectral temperature varies dramatically and the star exhibits a pronounced correlation between X-ray spectral temperature and luminosity. Fig. 5 shows the variation in the X-ray spectrum of a $1 M_{\odot}$ star produced by changes in the accretion rate. At low accretion rates, $\tau_{es} < 1$ and the observed hard X-ray spectrum is essentially that produced in the emission region. However, as the accretion rate is increased, τ_{es} exceeds unity and Compton scattering begins to degrade the spectrum. As the accretion rate is increased further, degradation of the spectrum becomes even more severe. Finally, due to the combined effects of degradation and weakening of the shock by radiation pressure, the bremsstrahlung component disappears altogether. The star then ceases

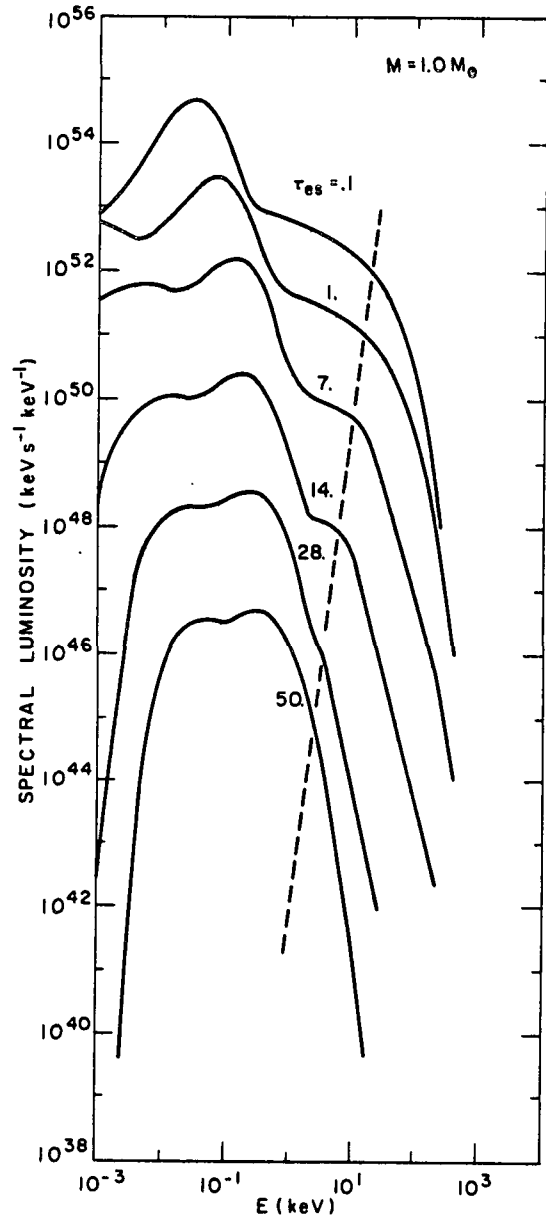


Fig. 5.- Variation in the X-ray and UV spectrum of a $1 M_{\odot}$ star produced by changes in the accretion rate and, therefore, τ_{es} . The six spectra shown correspond to accretion rates $\dot{M} = 1.1 \times 10^{-3}$, 1.1×10^{-2} , 7.8×10^{-2} , 0.15 , 0.27 , and $0.43 M_{\odot}$. The units on the vertical axis correspond to the $0.43 M_{\odot}$ ($\tau_{es} = 50$) curve. The other spectra have been multiplied by successively larger powers of 100 for clarity of presentation. The dashed line indicates the changing position of the hard X-ray cutoff produced by Compton scattering. (From Kylafis and Lamb 1979. By permission of The Astrophysical Journal.)

to be a hard ($T_{\text{obs}} > \text{keV}$) X-ray source.

The resulting correlation between T_{obs} and L_h is shown in Fig. 6 for stars with masses 0.2-1.2 M_{\odot} . The accretion rate increases as one moves from upper left to lower right along the curves. For sources found in the lower right of the Fig., an increase in T_{obs} and L_h therefore corresponds to a decrease in the accretion rate; T_{obs} and L_h increase since the smaller accretion rate lessens Compton degradation of the hard X-ray spectrum. A correlation like that in Fig. 6 is not expected for non-magnetic neutron stars and may be an important signature of degenerate dwarf X-ray sources.

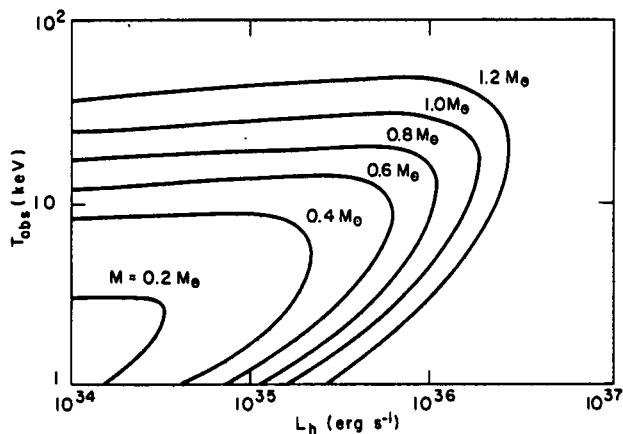


Fig. 6.- Correlation between T_{obs} and L_h for different mass stars. (From Kylafis and Lamb 1979. By permission of The Astrophysical Journal.)

This research has been supported in part by the NSF under Grant PHY78-04404 and by NASA under contract NAS5-24441. DQL gratefully acknowledges support from the John Simon Guggenheim Memorial Foundation.

REFERENCES

- Aizu, K. 1973, *Prog. Theoret. Phys.*, **49**, 1184.
- Fabian, A. C., Pringle, J. E., and Rees, M. J. 1976, *M.N.R.A.S.*, **173**, 43.
- Garmire, G. P. 1979, in Galactic Compact X-Ray Sources: Current Status and Future Prospects, ed. F. K. Lamb and D. Pines (University of Illinois, Urbana, Ill.).
- Hoshi, R. 1973, *Progr. Theoret. Phys.*, **49**, 776.
- Katz, J. I. 1977, *Ap. J.*, **215**, 265.
- Kylafis, N. D., and Lamb, D. Q. 1979, *Ap. J. (Letters)*, **228**, L105.
- Kylafis, N. D., Lamb, D. Q., Masters, A. R., and Weast, G. J. 1979, *Proc. Ninth Texas Symposium on Relativistic Astrophysics*, *Ann. N.Y. Acad. Sci.*, in press.
- Lamb, D. Q., and Masters, A. R. 1979, *Ap. J. (Letters)*, in press.
- Masters, A. R., Fabian, A. C., Pringle, J. E., and Rees, M. J. 1977, *M.N.R.A.S.*, **178**, 501.